THE JOURNAL OF PHYSICAL CHEMISTRY B LETTERS

2006, *110,* 9371−9374
Published on Web 04/22/2006

Low-Temperature Adsorption of Hydrogen on Nanoporous Aluminophosphates: Effect of Pore Size

Sung Hwa Jhung,* Hye-Kyung Kim, Ji Woong Yoon, and Jong-San Chang*

Research Center for Nanocatalysts, Korea Research Institute of Chemical Technology (KRICT), P.O. Box 107, Yusung, Daejeon 305-600, Korea

Received: February 28, 2006; In Final Form: March 29, 2006

Several nanoporous aluminophosphates (AlPOs) have been used to analyze the effect of pore diameter on the hydrogen adsorption characteristics. The heat of adsorption and adsorption capacity per unit micropore volume increase with decreasing pore size. AlPOs with smaller micropores favorably adsorb hydrogen at relatively low pressures. This work demonstrates that small pore size and large micropore volume are beneficial for high hydrogen uptake.

Efficient storage of hydrogen is very important for the utilization of hydrogen, one of the best alternative fuels for vehicles powered with fuel cells.[1,2] The storage of hydrogen via adsorption, including physisorption, using porous materials is one of several methods[3] currently being investigated. Porous materials such as carbons,[4,5] aluminosilicate zeolites,[6,7] and inorganic−organic hybrid materials[8−12] have been studied as potential hydrogen sorbents. Materials with high porosity (expressed either in terms of surface area or pore volume) are invariably sought due to the general consensus that higher porosity leads directly to higher overall hydrogen uptake.[1,3,7] To increase the adsorption capacity, several strategies such as (i) development of open or coordinatively unsaturated metal sites,[8,13] (ii) preparation of frameworks based on light metal species,[14] (iii) optimization of adsorption energy,[8] and (iv) utilization of hydrogen spillover[15] have been suggested. Acid−base, electrostatic, and dipole interactions have also been considered to be important.[16]

Very recently, by using isomorphous zinc dicarboxylate diamines (metal−organic porous materials), it has been demonstrated that the shape and size of a channel, rather than its chemical nature, significantly influence hydrogen adsorption.[17] Optimum pore size or small pore is stated to be important to enhance the hydrogen uptake.[8] Very small pores lead to high binding affinity due to increased van der Waals contact area.[14] Effective use of the available pore volume is most likely in materials with smaller pores.[18] Hysteresis in hydrogen adsorption and desorption occurs in a very small pore, which may not allow hydrogen to pass freely.[19] Several theoretical calculations have also been devoted to estimating the effect of pore size on the adsorption of hydrogen. For example, the binding force is calculated to decrease with increasing size of the carbon nanotubes.[20] High pressure or low temperature is needed for efficient adsorption on porous materials with large pores.[21]

However, to the best of our knowledge, the effect of pore size on the hydrogen sorption properties, including adsorption capacity, kinetics, energy, and so forth, has been never studied experimentally in detail. In particular, there have been no reports of hydrogen adsorption on porous materials with varying pore sizes but with similar surface areas, pore volume, architecture, and electrostatic field. Even though a quite detailed adsorption study has been carried out on isomorphous metal−organic porous materials by Chun et al.,[17] the chemical nature of ligands was different.

Aluminophosphate molecular sieves (AlPOs) with one-dimensional (1D) straight channels are an ideal set of materials for a systematic examination of the role of the pore size in hydrogen uptake, because many AlPOs with various pore sizes are known.[22] Moreover, AlPOs which have the same average chemical compositions of $AlPO_4$ do not have any charge compensating ion or strong acidity or basicity to influence the electrostatic field or interaction energy.

One-dimensional AlPOs with various pore sizes such as VPI-5[23] (18-membered ring (MR), IZA code[24] VFI), AlPO-5[25] (12 MR, IZA code MFI), AlPO-11[26] (10 MR, IZA code AEL), and AlPO-25[27] (8 MR, IZA code ATV) were synthesized hydrothermally from reactant gels under autogenous pressure by following the standard methods.[23,25−27] The gels made from alumina (psuedoboehmite), phosphoric acid, water, and a template were crystallized by microwave irradiation[28] to take advantage of fast crystallization or by conventional electric heating (for AlPO-21 which can be converted to AlPO-25 on calcination[27]). Di-*n*-propylamine, triethylamine, and pyrrolidine were used as templating agents for VPI-5 or AlPO-11, AlPO-5, and AlPO-21, respectively. Detailed synthetic conditions of AlPOs are summarized in Supporting Information Table 1. After crystallization, the AlPOs were recovered by cooling, filtration, washing, drying, and calcination. The phases and morphologies of AlPOs were analyzed by using XRD and SEM, respectively. AlPO-25 was obtained by in situ calcination of as-synthesized AlPO-21 (IZA code AWO) at 873 K for 6 h. The XRD patterns (Supporting Information Figure 1) agree well with those reported earlier.[23−27] The AlPOs thus obtained do not contain measurable impurities as confirmed by XRD and SEM images (Supporting Information Figure 2). To minimize the effect of crystal size

* Corresponding authors. Email: sung@krict.re.kr and jschang@krict.re.kr.

10.1021/jp061272c CCC: $33.50

TABLE 1: Physicochemical Properties of Various AlPOs and Summary of Their Hydrogen Adsorption Results

type of AlPOs	pore size (Å × Å)	S_{BET}[a] (m^2/g)	PV_μ[b] (mL/g)	V_{ads}[c] (mL/g)	ΔH_{ads}[d] (kJ/mol)	$P_{1/2}$[e] (Torr)	microore occupancy[f] (%)	surface coverage[g] (%)	$t_{1/2}$[h] (sec)	V_{ads}/S_{BET}[i] (mL/m^2)	V_{ads}/PV_μ[j]
VPI-5	12.7 × 12.7	327	0.126	37	−3.7	330	37.4	38.9	4.6	0.11	292
AlPO-5	7.3 × 7.3	297	0.114	46	−6.0	240	51.5	53.2	6.4	0.16	405
AlPO-11	6.5 × 4.0	222	0.103	44	−6.8	207	54.4	68.1	7.3	0.20	427
AlPO-25	4.9 × 3.0	220[k]	0.070[k]	44	−9.2	37	80.2	68.7	8.9	0.20	621

[a] Surface area calculated by the BET equation. [b] Micropore volume calculated by the Dubinin−Radushkevich equation. [c] Adsorption capacity of hydrogen at 760 Torr. The standard deviation of adsorption capacity by three experiments is less than 10%. [d] Heat of adsorption calculated by the Clausius−Clapeyron equation when the adsorbed amount is 15 mL/g. [e] The pressure at which half of adsorption capacity (at 760 Torr) is adsorbed. [f] Relative micropore occupancy by hydrogen calculated by using the density of liquid hydrogen (70.0 kg/m^3). [g] Relative surface coverage based on the fact that 1.3×10^{-5}mol of adsorbed hydrogen is needed to cover (monolayer) one square meter of a solid surface. [h] The time at which half of adsorption capacity (at infinite time) is adsorbed. [i] Relative adsorption capacity at 760 Torr per unit BET surface area. [j] Relative adsorption capacity at 760 Torr per unit micropore volume. [k] Determined with CO_2 adsorption because nitrogen is not adsorbed due to small pore size of AlPO-25.

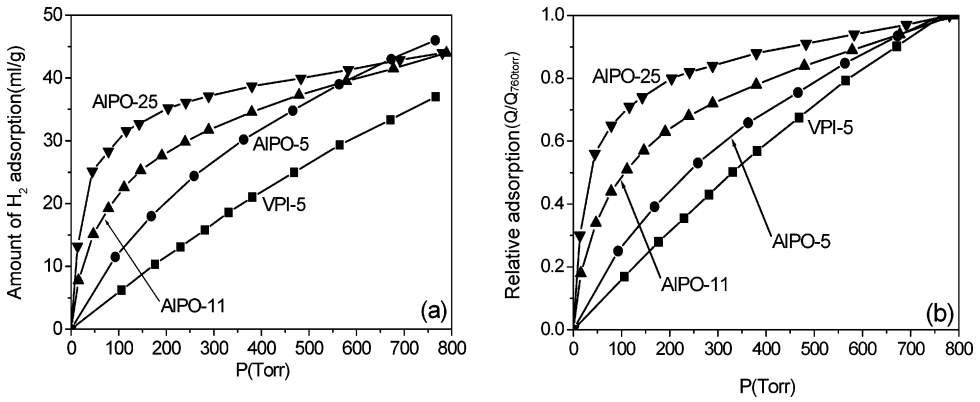

Figure 1. Hydrogen adsorption isotherms over various AlPOs at 77 K: (a) actual isotherms and (b) normalized isotherms.

on the adsorption kinetics and thermodynamics, all AlPOs were ground to fine powders whose images are shown in Supporting Information Figure 3. The surface area and micropore volume of various AlPOs were calculated from nitrogen adsorption isotherms by using BET and the Dubinin−Radushkevich equations, respectively. The nitrogen adsorption isotherms were obtained with a Micromeritics ASAP 2400 adsorption unit at liquid nitrogen temperature. The surface area and micropore volume of AlPO-25, after conversion from AlPO-21, were estimated by a CO_2 adsorption isotherm measured at 196 K using a homemade volumetric adsorption apparatus. The BET surface areas and micropore volumes are listed in Table 1. The sorption properties of AlPOs are similar to the previous results,[23−27] confirming the phase purity of the obtained samples in accordance with XRD and SEM results.

The H_2 adsorption on various AlPOs was also conducted using a homemade volumetric adsorption apparatus at liquid nitrogen (77 K) and liquid argon (87 K) temperatures. The adsorption capacities at various pressures were calculated using the ideal gas law, because the adsorption pressure was up to 760 Torr. The adsorption rates on AlPOs were compared with one another by the analysis of changes in hydrogen pressure from 150, 200, and 250 Torr to an equilibrium pressure. The accuracy of the adsorption unit for the measurement of the adsorption capacity was confirmed by conducting the experiments on the well-known molecular sieves such as ZSM-5 and SAPO-34.[29] The reproducibility of the adsorption data was confirmed at least three times, and the results shown in this study are averaged results derived from three independent experiments.

As shown in Figure 1 and Table 1, the AlPOs adsorb similar amounts of hydrogen at 760 Torr (37−46 mL/g). The desorption isotherms have the same characteristic line shapes as the adsorption isotherms (data not shown) which represents fully reversible adsorption due to physisorption. However, the uptake

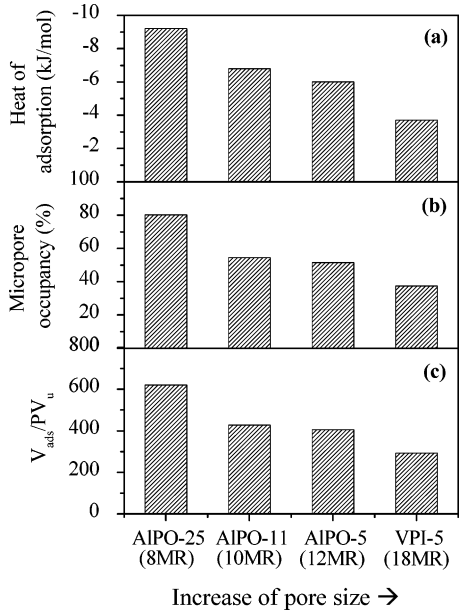

Figure 2. Effects of pore size of various AlPOs on (a) isosteric heat of adsorption, (b) micropore occupancy, and (c) relative adsorption capacity.

as a function of adsorption pressure varies considerably depending on the pore size. The pressures ($P_{1/2}$) at which half of the total adsorption capacity at 760 Torr is adsorbed are summarized in Table 1. Hydrogen adsorbs readily into micropores at a relatively low pressure with decreasing pore size from VPI-5 to AlPO-25, which presumably indicates an increase of interaction between hydrogen and narrow pores of AlPOs with smaller pore diameters.

The isosteric heat of adsorption (ΔH_{ads}) values calculated using the Clausius−Clapeyron[30] equation from the isotherms

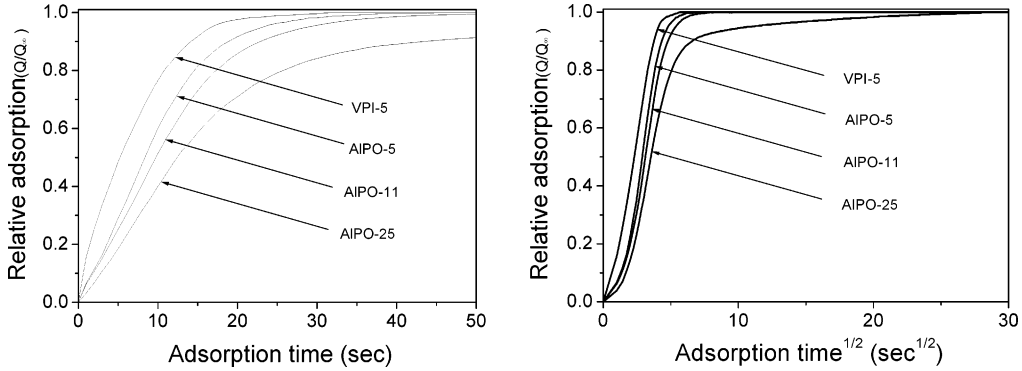

Figure 3. Hydrogen adsorption kinetics over various AlPOs at 77 K and 200 Torr. The ordinate scales are represented in time (s) and time$^{1/2}$ (s$^{1/2}$) in left and right figures, respectively. The adsorption kinetics does not depend on the initial hydrogen pressure from 150 to 250 Torr.

at 77 and 87 K are presented in Table 1, Figure 2a, and Supporting Information Figure 4. The absolute values for heat of adsorption steadily increases with decreasing pore size. This indicates that interactions between hydrogen and the framework structures increases when the pore size of AlPOs is small, which is consistent with the dependence of adsorption capacity on the relative pressure, as discussed above. Dinca and Long have found that the heat of adsorption on magnesium naphthalene-dicarboxylate is high (7.0−9.9 kJ/mol), which they attribute to very small pore size (3.46−3.64 Å) of the adsorbent.[14] Using computational methods, Efremenko and Sheintuch have also reported that the heat of adsorption decreases with increasing the size of carbon nanotubes.[20] Nevertheless, there have been no experimental results available to date which show the monotonic decrease of $-\Delta H_{ads}$ with increasing pore diameter in porous materials.

The relative occupancy of pore volume by the hydrogen molecule, calculated by using the liquid density of hydrogen (70.0 kg/m^3), increases from 37% to 80% with decreasing pore size of AlPOs (Table 1 and Figure 2b). High occupancy of hydrogen in very small micropores may be due to an increase of the interaction between hydrogen and the pore walls. The occupancy of adsorbed hydrogen on porous zinc dicarboxylate diamines ranges from 37% to 52%.[17] Similarly, the relative surface coverage increases from 39% to 69% with decreasing pore size (Table 1). The relative surface coverage, meaning the fraction of surface area that is covered by hydrogen, was calculated on the basis of the fact that 1.3×10^{-5} mol of adsorbed hydrogen is needed to cover one square meter of an adsorbent by monolayer.[1] The relative surface coverage is usually below 100% except for a porous hybrid material, manganese formate, whose coverage is 150%.[31] In our previous study, it was reported that the surface coverage values of zeolite Y, ZSM-5, and SAPO-34 were 66%, 32%, and 87%, respectively.[29] The levels of surface coverage of porous carbons and zeolites were reported to be 34% and 22%, respectively.[7]

As shown in Figure 3, all AlPOs rapidly adsorb hydrogen within 3 min, except for AlPO-25, which needs around 15 min to equilibrate. The times ($t_{1/2}$) at which half of the total adsorption capacity (at infinite time) is adsorbed are illustrated in Table 1. The adsorption rates increase slightly with increasing pore size (Figure 3), as might be anticipated. Even though the pore sizes are appreciably larger than the kinetic diameter[32] of hydrogen (2.89 Å), the adsorption rate in the pores of AlPOs depends on the pore diameter. For example, the adsorption in AlPO-25 (pore size: 4.9 Å × 3.0 Å) is greatly hindered and needs around 15 min for equilibration of each step in the adsorption experiments.

The relative adsorption capacities at 760 Torr per unit BET surface area or micropore volume increase with the decrease in pore size, as illustrated in Table 1 and Figure 2c. This confirms the increase in effectiveness of surface area or micropore volume on hydrogen storage with decreasing pore size. We have already reported that porous materials with small pores such as SAPO-34 and MIL-77 adsorb more hydrogen than other materials with similar surface areas or micropore volumes.[29] Pan et al. have also suggested that effective use of available pore volume is feasible for a material that has smaller pore size.[18] However, the relative effectiveness of smaller pores at higher pressures may be reduced, considering the decrease in slopes of the adsorption isotherms for AlPO-25 and AlPO-11 near 760 Torr. The effects of pore size on relative adsorption capacity per unit pore volume, micropore occupancy, and isosteric heat of adsorption ($-\Delta H_{ads}$) are summarized in Figure 2.

In summary, we have experimentally demonstrated for the first time that the relative adsorption capacities per unit micropore volume or BET surface area increase with decreasing pore size of an adsorbent. Moreover, the isosteric heat of adsorption is high and the adsorption occurs readily at relatively low pressure for porous materials with small pore size. Therefore, it is reasonable to suggest that the idealized porous material for an efficient hydrogen storage, especially at low pressure, is one with narrow pores and large micropore volume, or large surface area.

Acknowledgment. This work was supported by Institutional Research Program (KK-0603-F0) and the Korea Ministry of Science and Technology through International Collaboration Research Program (KN-0533). The authors thank Dr. M. K. Song (BMD), Dr. D. P. Amalnerkar (C-MET), and Dr. A. S. Mamman (NCL) for helpful discussions, and Dr. P. M. Forster (Stony Brook University) and Dr. S. M. Humphery (University of California, Berkeley) for helpful comments.

Supporting Information Available: Structures and synthesis conditions of various AlPOs, XRD patterns and SEM images of various AlPOs, and heat of adsorption values. This material is available free of charge via the Internet at http://pubs.acs.org.

References and Notes

(1) Schlapbach, L.; Züttel, A. *Nature (London)* **2001**, *414*, 353.
(2) Seayad, A. M.; Antonelli, D. M. *Adv. Mater.* **2004**, *16*, 765.
(3) Züttel, A. *Mater. Today* **2003**, *6*, 24.
(4) Darkrim, F. L.; Malbrunot, P.; Tartaglia, G. P. *Int. J. Hydrogen Energy* **2002**, *27*, 193.
(5) Dillon, A. C.; Heben, M. J. *Appl. Phys. A* **2001**, *72*, 133.

(6) Zecchina, A. A.; Bordiga, S.; Vitillo, J. G.; Ricchiardi, G.; Lamberti, C.; Spoto, G.; Bjørgen, M.; Lillerud, K. P. *J. Am. Chem. Soc.* **2005**, *127*, 6361.

(7) Nijkamp, M. G.; Raaymakers, J. E. M. J.; van Dillen, A. J.; de Jong, K. P. *Appl. Phys. A* **2001**, *72*, 619.

(8) Rowsell, J. L. C.; Yaghi, O. M. *Angew. Chem., Int. Ed.* **2005**, *44*, 4670.

(9) (a) Férey, G.; Latroche, M.; Serre, C.; Millange, F.; Loiseau, T.; Percheron-Guégan, A. *Chem. Commun.* **2003**, 2976. (b) Lee, E. Y.; Suh, M. P. *Angew. Chem., Int. Ed.* **2004**, *43*, 2798. (c) Kesanli, B.; Cui, Y.; Smith, M. R.; Bittner, E. W.; Bockrath, B. C.; Lin, W. *Angew. Chem., Int. Ed.* **2005**, *44*, 72.

(10) Chen, B.; Ockwig, N. W.; Millward, A. R.; Contreras, D. S.; Yaghi, O. M. *Angew. Chem., Int. Ed.* **2005**, *44*, 4745.

(11) Rowsell, J. L. C.; Spencer, E. C.; Eckert, J.; Howard, J. A. K.; Yaghi, O. M. *Science* **2005**, *309*, 1350.

(12) Rowsell, J. L. C.; Millward, A. R.; Park, K. S.; Yaghi, O. M. *J. Am. Chem. Soc.* **2004**, *126*, 5666.

(13) (a) Forster, P. M.; Eckert, J.; Chang, J.-S.; Park, S.-E.; Férey, G.; Cheetham, A. K. *J. Am. Chem. Soc.* **2003**, *125*, 1309. (b) Yang, Q.; Zhong, C. *J. Phys. Chem. B* **2006**, *110*, 655.

(14) Dincă, M.; Long, J. R. *J. Am. Chem. Soc.* **2005**, *127*, 9376.

(15) Li, Y.; Yang, R. T. *J. Am. Chem. Soc.* **2006**, *128*, 726.

(16) (a) Kazansky, V. B.; Borovkov, V. Yu.; Serich, A.; Karge, H. G. *Microporous Mesoporous Mater.* **1998**, *22*, 251. (b) Froudakis, G. E. *Nano Lett.* **2001**, *1*, 531.

(17) Chun, H.; Dybtsev, D. N.; Kim, H.; Kim, K. *Chem.—Eur. J.* **2005**, *11*, 3521.

(18) Pan, P.; Sander, M. B.; Huang, X.; Li, J.; Smith, M.; Bittner, E.; Bockrath, B.; Johnson, J. K. *J. Am. Chem. Soc.* **2004**, *126*, 1308.

(19) Zhao, X.; Xiao, B.; Fletcher, A.; Thomas, K. M.; Bradshaw, D.; Rosseinsky, M. J. *Science* **2004**, *306*, 1012.

(20) Efremenko, I.; Sheintuch, M. *Langmuir* **2005**, *21*, 6282.

(21) Rzepka, M.; Lamp, P.; de la Casa-Lillo, M. A. *J. Phys. Chem. B* **1998**, *102*, 10894.

(22) Wilson, S. T. *Stud. Surf. Sci. Catal.* **2001**, *137*, 229.

(23) Carmona, J. G.; Clemente, R. R.; Morales, J. G. *Zeolites* **1997**, *18*, 340.

(24) http://topaz.ethz.ch/IZA-SC/StdAtlas.htm.

(25) (a) Jhung, S. H.; Chang, J.-S.; Hwang, Y. K.; Park, S.-E. *J. Mater. Chem.* **2004**, *14*, 280. (b) Jhung, S. H.; Hwang, Y. K.; Chang, J.-S.; Park, S.-E. *Microporous Mesoporous Mater.* **2004**, *67*, 151.

(26) (a) Strohmaier, K. G.; Vaughan, D. E. W. U.S. Patent 6,303,534 B1, 2001. (b) Alfonzo, M.; Goldwasser, J.; López, C. M.; Machado, F. J.; Matjushin, M.; Méndez, B.; de Agudelo, M. M. R. *J. Mol. Catal., A* **1995**, *98*, 35.

(27) (a) Wilson, S. T.; Lok, B. M.; Flanigem, E. M. U.S. Patent 4,-310,440, 1982. (b) Li, J.; Yu, J.; Zhu, G.; Xu, R. *Inorg. Chem.* **2001**, *40*, 5812.

(28) (a) Tompsett, G.; Conner, W. C.; Yngvesson, K. S. *ChemPhysChem* **2006**, *7*, 296. (b) Park, S.-E.; Chang, J.-S.; Hwang, Y. K.; Kim, D. S.; Jhung, S. H.; Hwang, J.-S. *Catal. Surv. Asia* **2004**, *8*, 91. (c) Jhung, S. H.; Yoon, J. W.; Hwang, J.-S.; Cheetham, A. K.; Chang, J.-S. *Chem. Mater.* **2005**, *17*, 4455.

(29) Jhung, S. H.; Yoon, J. Y.; Kim, H.-K.; Chang, J.-S. *Bull. Kor. Chem. Soc.* **2005**, *26*, 1075.

(30) Thomas, J. M.; Thomas, W. J. *Introduction to the Principles of Heterogeneous Catalysis*; Academic Press: New York, 1967; p 102.

(31) Dybtsev, D. N.; Chun, H.; Yoon, S. H.; Kim, D.; Kim, K. *J. Am. Chem. Soc.* **2004**, *126*, 32.

(32) Breck, D. W. *Zeolite Molecular Sieves*; John Wiley & Sons: New York, 1974; p 634.